Downstream changes in river avulsion style are related to channel morphology

Valenza et al.

Contents

SUPPLEMENTARY MATERIAL

Avulsion ID	Lat	Lon	type	River distance (km)	Channel width (m)	Normalized distance	Channel-belt slope	Avulsion style ratio (S_R)	Link to avulsion location in Google Earth Engine
V1	1.10920	-76.23480	1	7.1	198	35.9	0.00353	1.0	https://earthengine.google.org/#timelapse/v=1.1092,-76.2348,11.4,latLng
V4	3.50400	-73.87590	1	16.1	432	37.3	0.01100	1.9	https://earthengine.google.org/#timelapse/v=3.504,-73.8759,11.4,latLng
V5_1	3.74260	-73.54850	2	35.4	147	240.8	0.00375	0.6	https://earthengine.google.org/#timelapse/v=3.7426,-73.5485,11.4,latLng
V5_2	3.73056	-73.49434	2	41.9	138	303.6	0.00381	1.1	https://earthengine.google.org/#timelapse/v=3.730559,-73.494341,11.4,latLng
V6	6.19340	-71.77800	1	29.2	595	49.1	0.01028	1.8	https://earthengine.google.org/#timelapse/v=6.1934,-71.778,11.4,latLng
V7	6.73000	-71.25650	3	69.9	57	1226.3	0.00115	11.4	https://earthengine.google.org/#timelapse/v=6.73,-71.2565,11.4,latLng
V8	6.94976	-71.98327	1	13.9	349	39.8	0.01419	1.3	https://earthengine.google.org/#timelapse/v=6.94976,-71.98327,11.4,latLng
V9	7.03724	-72.04633	1	13.3	677	19.6	0.00777	1.2	https://earthengine.google.org/#timelapse/v=7.03724,-72.04633,11.4,latLng
V10	7.07250	-72.00890	2	15.5	89	174.2	0.01923	1.0	https://earthengine.google.org/#timelapse/v=7.0725,-72.0089,11.4,latLng
V11	7.17030	-71.34500	3	82.4	110	749.1	0.00058	16.0	https://earthengine.google.org/#timelapse/v=7.1703,-71.345,11.4,latLng
V12_1	7.49590	-72.03500	1	4.8	150	32.0	0.01950	0.8	https://earthengine.google.org/#timelapse/v=7.4959,-72.035,11.4,latLng
V12_2	7.49590	-72.03500	1	4.8	150	32.0	0.01950	1.4	https://earthengine.google.org/#timelapse/v=7.4959,-72.035,11.4,latLng
V12_3	7.49590	-72.03500	1	4.8	150	32.0	0.01950	1.3	https://earthengine.google.org/#timelapse/v=7.4959,-72.035,11.4,latLng
V13	7.55960	-72.07990	1	1.8	670	2.7	0.07698	0.7	https://earthengine.google.org/#timelapse/v=7.5596,-72.0799,11.4,latLng
V14	8.41460	-69.98310	3	69.7	90	774.4	0.00146	25.4	https://earthengine.google.org/#timelapse/v=8.4146,-69.9831,11.4,latLng
V15	7.23583	-71.94778	1	16.9	426	39.7	0.02400	0.5	https://earthengine.google.org/#timelapse/v=7.23583,-71.94778,11.4,latLng
B1	-17.08150	-62.97950	3	249.0	400	622.5	0.00049	38.9	https://earthengine.google.org/#timelapse/v=-17.0815,-62.9795,11.4,latLng
B2	-17.42410	-64.13510	3	4.1	60	68.3	0.01500	0.4	https://earthengine.google.org/#timelapse/v=-17.4241,-64.1351,11.4,latLng
B3	-17.37140	-64.21650	1	7.3	530	13.8	0.04889	1.1	https://earthengine.google.org/#timelapse/v=-17.3714,-64.2165,11.4,latLng
B4	-17.21600	-64.85500	1	8.6	888	9.7	0.01460	1.5	https://earthengine.google.org/#timelapse/v=-17.216,-64.855,11.4,latLng
B6	-16.97290	-65.39850	1	1.3	1540	0.9	0.00366	1.0	https://earthengine.google.org/#timelapse/v=-16.9729,-65.3985,11.4,latLng

B7	-16.70480	-65.65000	3	3.1	132	23.5	0.03263	0.9	https://earthengine.google.org/#timelapse/v=-16.7048,-65.65,11.4,latLng
B8	-16.61250	-65.74380	2	2.5	113	22.1	0.00596	1.1	https://earthengine.google.org/#timelapse/v=-16.6125,-65.7438,11.4,latLng
B9	-16.32250	-65.83840	3	60.8	159	382.4	0.00103	3.3	https://earthengine.google.org/#timelapse/v=-16.3225,-65.8384,11.4,latLng
B10	-16.27280	-65.20380	3	82.9	164	505.5	0.00068	13.9	https://earthengine.google.org/#timelapse/v=-16.2728,-65.2038,11.4,latLng
B11	-16.06620	-66.15720	3	19.1	38	502.6	0.00212	1.5	https://earthengine.google.org/#timelapse/v=-16.0662,-66.1572,11.4,latLng
B12	-15.87900	-65.85900	3	49.5	98	505.1	0.00075	12.8	https://earthengine.google.org/#timelapse/v=-15.879,-65.859,11.4,latLng
B13	-15.86680	-66.36140	3	10.4	112	92.9	0.00306	0.8	https://earthengine.google.org/#timelapse/v=-15.8668,-66.3614,11.4,latLng
B14	-14.67700	-66.53080	3	134.0	110	1218.2	0.00021	53.7	https://earthengine.google.org/#timelapse/v=-14.677,-66.5308,11.4,latLng
B15	-23.07690	-64.31870	1	19.3	355	54.4	0.00295	1.0	https://earthengine.google.org/#timelapse/v=-23.0769,-64.3187,11.4,latLng
H1	27.41970	94.24130	1	14.9	369	40.4	0.00059	0.9	https://earthengine.google.org/#timelapse/v=27.4197,94.2413,11.4,latLng
H2	27.67860	94.85750	1	9.1	176.5	51.6	0.00081	2.0	https://earthengine.google.org/#timelapse/v=27.6786,94.8575,11.4,latLng
H3	26.91380	86.04600	1	2.3	121	19.0	0.00682	1.2	https://earthengine.google.org/#timelapse/v=26.9138,86.046,11.4,latLng
H4	29.38049	78.89051	1	7.8	70	111.4	0.00441	0.8	https://earthengine.google.org/#timelapse/v=29.380488,78.890506,11.4,latLng
H5	26.78360	90.95660	1	0.4	1500	0.3	0.00165	0.8	https://earthengine.google.org/#timelapse/v=26.7836,90.9566,11.4,latLng
H6	27.49620	96.21850	1	17.1	980	17.4	0.00383	1.4	https://earthengine.google.org/#timelapse/v=27.4962,96.2185,11.4,latLng
G1	-5.72600	145.52700	2	59.5	154	386.4	0.00187	2.2	https://earthengine.google.org/#timelapse/v=-5.726,145.527,11.4,latLng
G2	-5.15780	144.78870	2	8.1	37.6	215.4	0.00255	9.5	https://earthengine.google.org/#timelapse/v=-5.1578,144.7887,11.4,latLng
G3	-9.64820	148.73160	2	3.1	111	27.9	0.00375	1.2	https://earthengine.google.org/#timelapse/v=-9.6482,148.7316,11.4,latLng
G4	-9.62060	148.65000	2	3.2	24	132.9	0.00494	1.6	https://earthengine.google.org/#timelapse/v=-9.6206,148.65,11.4,latLng
G5	-4.15120	135.24400	2	8.6	360	23.9	0.00452	4.9	https://earthengine.google.org/#timelapse/v=-4.1512,135.244,11.4,latLng
G6	-3.96930	135.21810	1	4.1	330	12.6	0.01113	0.7	https://earthengine.google.org/#timelapse/v=-3.9693,135.2181,11.4,latLng
G7	-4.00730	135.25140	1	0.1	87.4	1.1	0.01507	1.5	https://earthengine.google.org/#timelapse/v=-4.0073,135.2514,11.4,latLng
G8	-3.96860	135.07490	3	22.2	82	270.2	0.00334	13.1	https://earthengine.google.org/#timelapse/v=-3.9686,135.0749,11.4,latLng
G9	-3.04910	136.37110	1	6.3	124	51.1	0.00501	1.5	https://earthengine.google.org/#timelapse/v=-3.0491,136.3711,11.4,latLng
G10	-3.35350	138.75940	2	6.3	59	106.1	0.01534	0.5	https://earthengine.google.org/#timelapse/v=-3.3535,138.7594,11.4,latLng
G11	-6.57620	146.69910	1	9.7	219	44.3	0.00487	0.7	https://earthengine.google.org/#timelapse/v=-6.5762,146.6991,11.4,latLng

G12	-6.66240	147.05690	2	4.0	148	27.0	0.01329	2.5	https://earthengine.google.org/#timelapse/v=-6.6624,147.0569,11.4,latLng
G13	-6.69530	147.21110	1	4.0	231	17.3	0.01132	1.7	https://earthengine.google.org/#timelapse/v=-6.6953,147.2111,11.4,latLng
G14	-6.69310	147.33000	1	2.3	405	5.7	0.01616	0.7	https://earthengine.google.org/#timelapse/v=-6.6931,147.33,11.4,latLng
G15	-7.57740	147.23590	1	0.1	168	0.6	0.00469	0.7	https://earthengine.google.org/#timelapse/v=-7.5774,147.2359,11.4,latLng
G16	-7.67100	147.42650	2	3.1	182	17.0	0.00226	1.0	https://earthengine.google.org/#timelapse/v=-7.671,147.4265,11.4,latLng
G17	-9.07900	149.04070	1	5.7	215	26.5	0.00410	1.4	https://earthengine.google.org/#timelapse/v=-9.079,149.0407,11.4,latLng
G18	-9.62930	149.30820	1	6.5	220	29.5	0.00947	0.9	https://earthengine.google.org/#timelapse/v=-9.6293,149.3082,11.4,latLng
G19	-4.97120	139.91190	1	7.4	137	54.0	0.00502	0.9	https://earthengine.google.org/#timelapse/v=-4.9712,139.9119,11.4,latLng
G20	-5.06240	139.72730	3	22.9	96	238.5	0.00330	1.7	https://earthengine.google.org/#timelapse/v=-5.0624,139.7273,11.4,latLng
G21	-4.72310	139.30090	1	7.0	752	9.3	0.00499	0.7	https://earthengine.google.org/#timelapse/v=-4.7231,139.3009,11.4,latLng
G22	-4.68700	138.78890	2	6.7	164	40.9	0.00138	1.6	https://earthengine.google.org/#timelapse/v=-4.687,138.7889,11.4,latLng
G23	-4.36630	136.84750	1	9.7	290	33.4	0.00509	0.6	https://earthengine.google.org/#timelapse/v=-4.3663,136.8475,11.4,latLng
G24	-4.34880	136.79780	1	6.4	360	17.8	0.00758	1.2	https://earthengine.google.org/#timelapse/v=-4.3488,136.7978,11.4,latLng
G25_1	-0.76726	133.62207	2	8.9	110	81.0	0.01113	1.0	https://earthengine.google.org/#timelapse/v=-0.767259,133.622071,11.4,latLng
G25_2	-0.80550	133.62000	1	5.4	310	17.4	0.01130	0.7	https://earthengine.google.org/#timelapse/v=-0.8055,133.62,11.4,latLng
G26	-3.31720	128.68310	3	1.5	205	7.3	0.00364	0.6	https://earthengine.google.org/#timelapse/v=-3.3172,128.6831,11.4,latLng

Supplementary Table 1. **Avulsion Style data**. Type refers to channel morphology as 1 – multithreaded, 2 – transitional, and 3 – single threaded. Normalized distance is the river distance (mountain front to avulsion site) divided by channel width.

Landsat 5	Band 1	Band 2	Band 3	Band 4	Band 5	Band 7
	0.2909	0.2493	0.4806	0.5568	0.4438	0.1706
	-0.2728	-0.2174	-0.5508	0.7221	0.0733	-0.1648
	0.1446	0.1761	0.3322	0.3396	-0.621	-0.4186
	0.8461	-0.0731	-0.464	-0.0032	-0.0492	0.0119
	0.0549	-0.0232	0.0339	-0.1937	0.4162	-0.7823
	0.1186	-0.8069	0.4094	0.0571	-0.0228	0.022
Landsat 7	Band 1	Band 2	Band 3	Band 4	Band 5	Band 7
	0.3561	0.3972	0.3904	0.6966	0.2286	0.1596
	-0.3344	-0.3544	-0.4556	0.6966	-0.0242	-0.263
	0.2626	0.2141	0.0926	0.0656	-0.7629	-0.5388
	0.0805	-0.0498	0.195	-0.1327	0.5752	-0.7775
	-0.7252	-0.0202	0.6683	0.0631	-0.1494	-0.0274
	0.4	-0.8172	0.3832	0.0602	-0.1095	0.0985
Landsat 8	Band 1	Band 2	Band 3	Band 4	Band 5	Band 7
	0.3029	0.2786	0.4733	0.5599	0.508	0.1872
	-0.2941	-0.243	-0.5424	0.7276	0.0713	-0.1608
	0.1511	0.1973	0.3283	0.3407	-0.7117	-0.4559
	-0.8239	0.0849	0.4396	-0.058	0.2013	-0.2773
	-0.3294	0.0557	0.1056	0.1855	-0.4349	0.8085
	0.1079	-0.9023	0.4119	0.0575	-0.0259	0.0252

Supplementary Table 2. **Tasseled-cap coefficients**. Different sets of coefficients were derived for different landsat missions: Landsat 4-5 (ref. 1). Landsat 7 (ref. 2), and Landsat 8 (ref. 3). Coefficients are used to process band data to compress the multiple Landsat bands into three physically meaningful bands, including brightness, greenness, and wetness.

Supplementary Figures

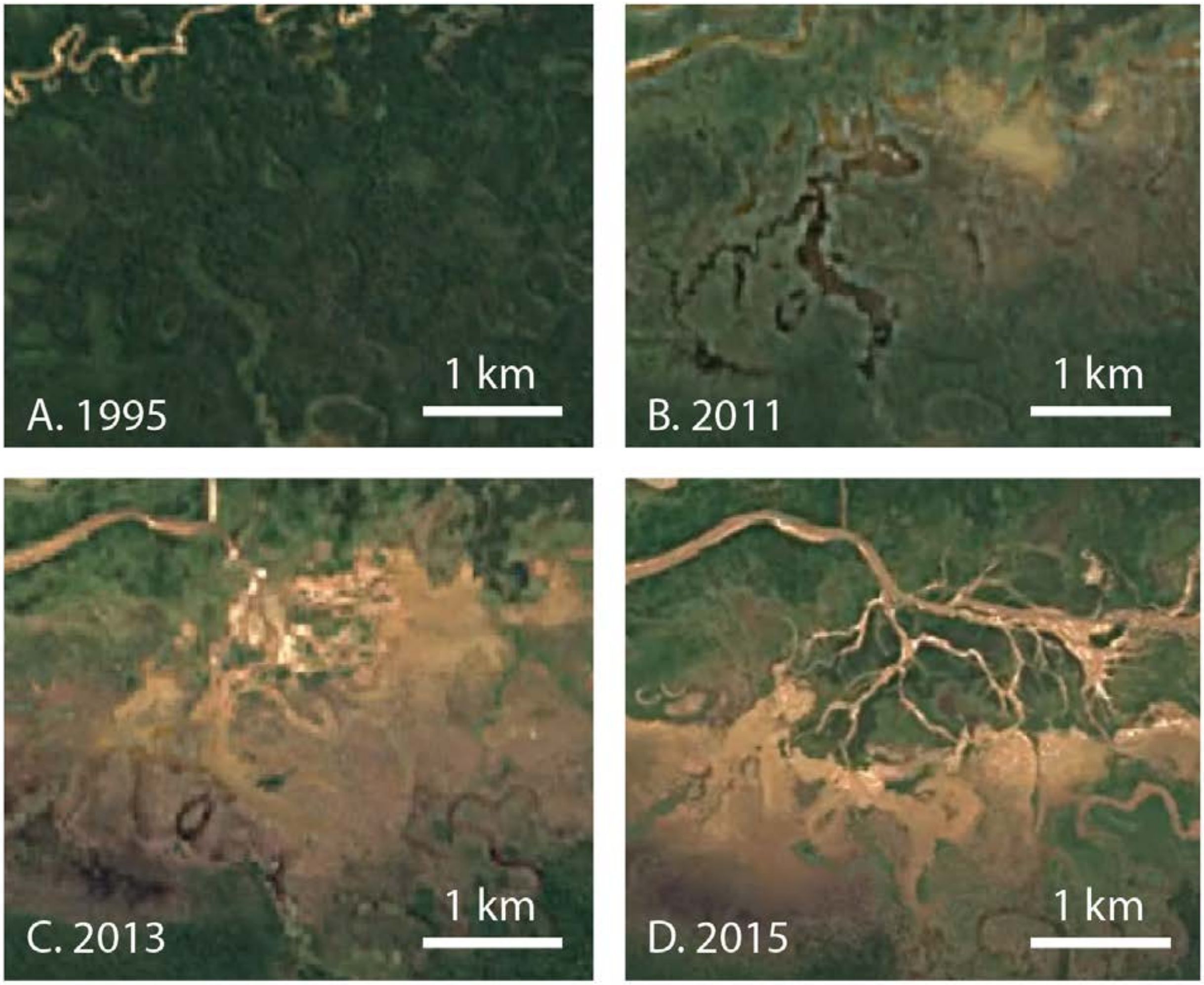

Supplementary Figure 1. **Progression of land surface changes during progradational event (sample B12, Bolivia)**. Changes in color correspond to shifts in the land surface spectra. A. undisturbed forest and parent channel (1995). B. Initial diversion of flow from parent channel results in flooding, in this case without a crevasse splay (2011). C. Incipient distributary network and expanding flooding area with vegetation removal (2013). D. Further development of distributary network and strengthening of a single distributary channel (2015). Annual composite images from www.earthengine.google.com/timelapse.

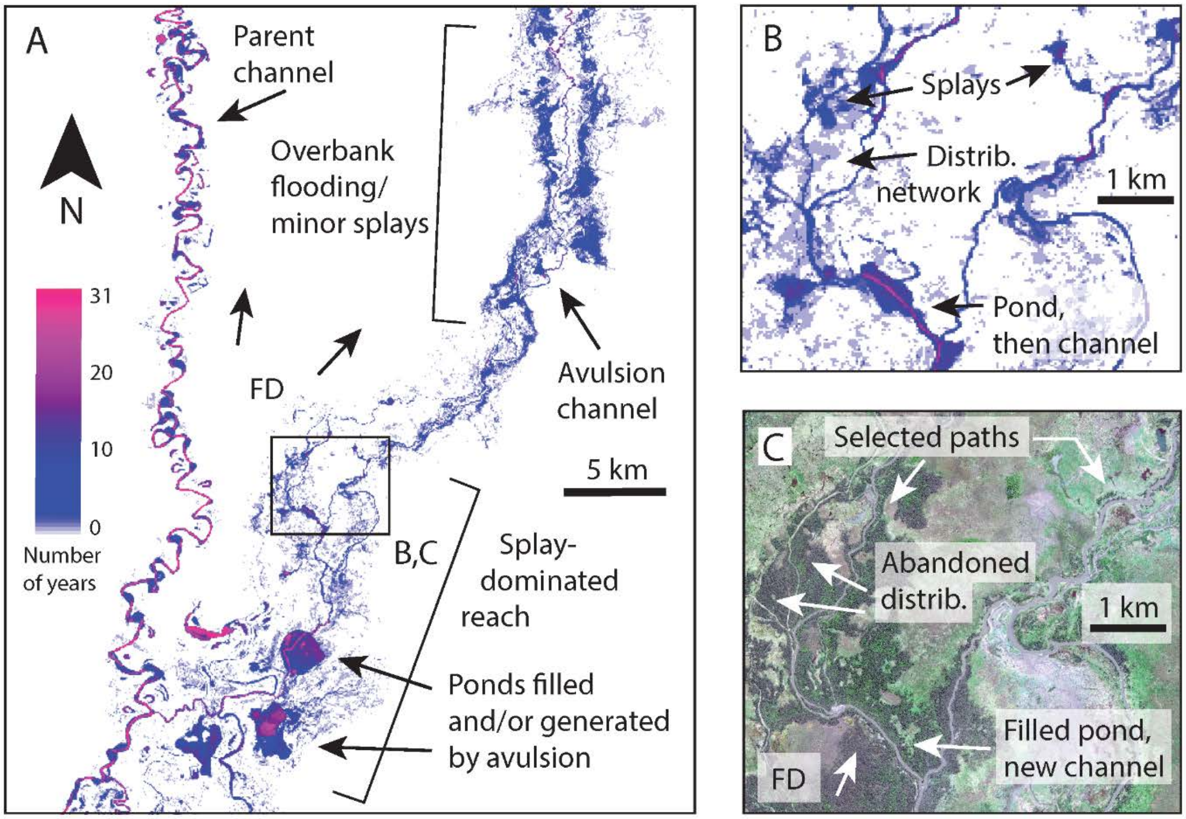

Supplementary Figure 2. Qualitative validation of results from avulsion sample B11, Bolivia. A. Avulsion fingerprint, where positively identified avulsion pixels from each annual composite are summed, constituting the "number of years", pink representing more years of activity, blue, fewer. Flow direction (FD) is to the north for the parent channel and to northeast for the avulsion channel. Two distinct reaches are visible, with the first dominated by splays and pond generation and filling, followed downstream by annexation accompanied by proximal overbank flooding and minor splays. B. Subset of avulsion fingerprint within splay dominated reach showing morphological details including splays, distributary network, and ponding. C. High-resolution image of the same subset area, July 8, 2016. Selected and abandoned channel flow paths are annotated. Note areas covered by splays are later colonized by dense vegetation (dark green). World View 1 RGB image from Digital Globe.

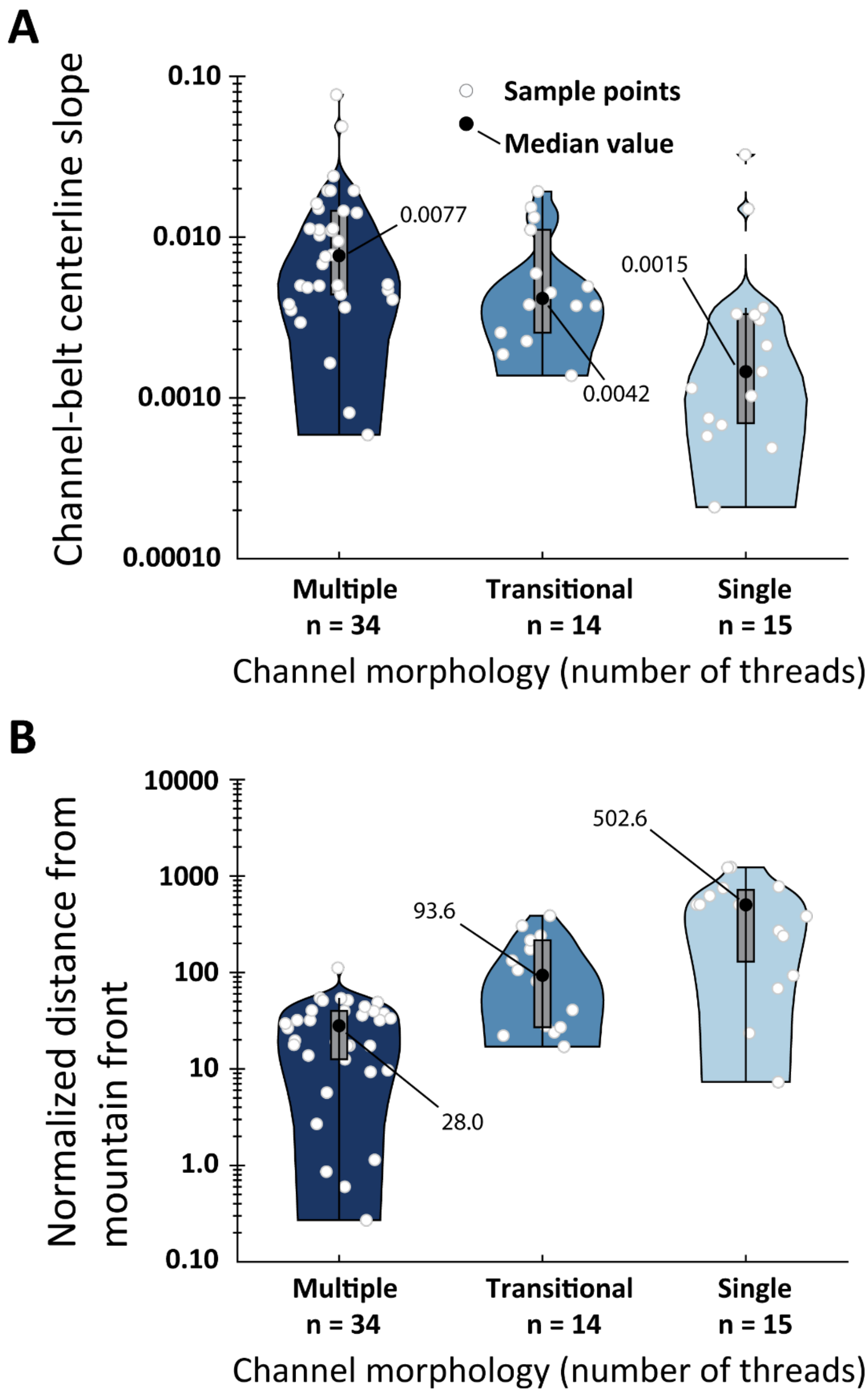

Supplementary Figure 3. Channel morphology is related to slope and normalized distance. Avulsion sites are used as points of reference for the following comparisons of channel characteristics: A. Channel morphologies exhibit unique distributions and medians for slope along the channel belt centerline. Multithread channels have the highest median value at 0.0077, and show the most skew towards higher slope values. Events in transitional channels have median S_R value of 0.0042, with the least skew. Single-thread channels have the lowest median value at 0.0015. B. Channel morphologies exhibit even more discrete distributions and medians for normalized distance (length/width) from the mountain front. Multithread channels have the lowest median distance value of 28.0, transitional channels again have a value of 93.6, and single-thread channels have the highest median distance value of 502.6. These trends follow the simple generalization that rivers tend to exhibit multithread morphology in more proximal locations with higher slopes, and single-thread morphology in more distal locations with lower slopes. Numbers refer to median values of the distributions, boxes show the 2nd to 3rd quartile ranges, and lines extending from boxes represent the 1st to 2nd and 3rd to 4th quartile ranges.

References

1 Kauth, R. J. & Thomas, G. in *LARS symposia*. 159.

2 Crist, E. P. & Cicone, R. C. A physically-based transformation of Thematic Mapper data---The TM Tasseled Cap. *IEEE Transactions on Geoscience Remote Sensing*, 256-263 (1984).

3 Baig, M. H. A., Zhang, L., Shuai, T. & Tong, Q. Derivation of a tasselled cap transformation based on Landsat 8 at-satellite reflectance. *Remote Sensing Letters* **5**, 423-431 (2014).